



IMPROVING THE SEISMIC PERFORMANCE OF EXISTING BRIDGE STRUCTURES USING SELF-CENTERING DAMPERS

X. Cheng⁽¹⁾, J. Erochko⁽²⁾, D.T. Lau⁽³⁾

⁽¹⁾ Graduate Student, Dept. of Civil & Environmental Engineering, Carleton University, Ottawa, Canada,
Email: xicheng3@carleton.ca

⁽²⁾ Assistant Professor, Dept. of Civil & Environmental Engineering, Carleton University, Ottawa, Canada,
Email: Jeffrey.Erochko@carleton.ca

⁽³⁾ Professor, Dept. of Civil & Environmental Engineering, Carleton University, Ottawa, Canada,
Email: David.Lau@carleton.ca

Abstract

Self-centering (SC) systems are relatively new seismic resistant structural systems that reduce or eliminate the residual drifts and deformations of structures caused by earthquakes. In engineering practice, although some of the earliest applications of self-centering systems were in bridges, the majority of existing self-centering systems are for building applications to increase the chance that the building will still be serviceable after an earthquake. Bridge structures can suffer similar excessive drifts or residual displacements in earthquakes, which can result in lengthy traffic closures, costly repair or even demolition after an earthquake. The goal of this study is to improve bridge performance by using a self-centering lateral load resisting cross brace element that was designed originally for use in buildings. This brace, the self-centering energy-dissipative (SCED) brace may be applied to a bridge as a retrofit solution, unlike many other currently used self-centering bridge systems which require rocking piers. This is especially important since the vast majority of necessary bridges are already built and many of them are currently deficient. The benefits of employing the self-centering brace to retrofit two seismically deficient bridges are investigated. The bridges are modeled using OpenSEES and are subjected to simulated earthquakes at the maximum credible hazard level. The performance of the self-centering retrofitted bridges are evaluated and compared with those of the original structures. The results demonstrate the self-centering brace systems are effective in reducing the maximum drift and eliminating the residual displacement of the bridges during and after the seismic events.

Keywords: Self-centering, Retrofit, Bridges, Reinforced Concrete, Seismic Performance

1. Introduction

Recent earthquakes (e.g. 2010 Chile; 1995 Kobe, Japan; 1994 Northridge, California) have shown that many existing old bridges constructed prior to 1970s before the adoption of the current more stringent seismic design standards and practices are vulnerable to earthquake damage. As such, there is a need to develop effective seismic retrofit techniques for improving the resistance as well as the performance of these seismically deficient structures.

As noted by Priestley [1], a large part of the highway systems in many countries were constructed before the current level of understanding about how they would behave during earthquakes. In general, it is accepted that the observations of bridge performance during the 1971 San Fernando, California [2] and 1989 Loma Prieta, California earthquakes have led to significant advances in the seismic design approach and practice for bridges [2]. Consequently, bridges constructed before the 1970s are particularly vulnerable to seismic damage. In Canada, there are over 50,000 existing bridges and a significant number of those were constructed in the 1960s and 1970s. As shown in previous literature, in general these older bridges do not have the strength, ductility and resilience to resist expected seismic load and displacement demands [3].

Compared to buildings, bridge structures typically have much less or no redundancy. This means that progressive failure initiated from one structural member or components can lead to collapse or severe damage to the entire structure. In the past, earthquake resistant design of structures has primarily focused only on life safety. When this design philosophy is applied to bridges, the significant inelastic deformations suffered by the

bridge piers often lead to large residual displacements at the abutment approaches or expansion joints of the bridge. Any large differential residual displacements at abutment approaches would likely force the closure of the bridge to vehicle traffic immediately after the earthquakes even though the structures may be deemed safe to carry the associated gravity load. Particularly for those designated as lifeline bridges, there is the strong need to improve their resilience by reducing the risk of downtime. One potential approach to reduce the likelihood of this happening is to add self-centering braces between the piers and superstructure to add energy dissipation and provide a re-centering mechanism to prevent bridge alignment problems.

In combination with this, the use of performance-based earthquake engineering can be used to achieve more tailored bridge performance for each different earthquake hazard level. With increasing confidence that modern structures can now reliably achieve life-safety performance level, there is now considerable research into reducing structural damage under moderate earthquakes [4]. Self-centering (SC) systems may be used to purposefully increase structural performance at these more moderate hazard levels. For bridge structures, recent research efforts in self-centering systems have focused mainly on post-tensioned rocking pier mechanisms [5,6,7]; however, such self-centering systems are difficult or impractical to implement for the retrofit of existing bridges. To address these drawbacks, SCED braces [4,5], previously developed for applications in buildings, are adapted here for use in the retrofit of existing bridges. When deformed, the self-centering energy-dissipative (SCED) braces generate large restoring forces that can help the structure to return to the neutral position thus minimizing or eliminating residual deformations and enhancing the serviceability of the structure following a seismic event. This study investigates the performance of two sample seismically deficient concrete bridges, which are retrofitted using SCED braces.

2. Self-centering Systems

As discussed by Christopoulos and Filiatrault [8], an ideal seismic resistant system should be able to dissipate energy and return to its original position with main structural elements undamaged after an earthquake. By comparing the behavior of a conventional structural system and one supplemented with a SC system from a qualitative perspective, several differences in their behaviour may be observed as shown in Fig. 1. The SC system has less energy dissipated but more frequent stiffness changes per cycle compared with the conventional system. The most attractive feature of the SC system is that it returns to zero-force and zero-displacement point at every cycle whereas the conventional system leads to cumulative deformation at every cycle.



Fig. 1 - Idealized Force-Displacement Relationship: (a) Conventional Hysteresis; (b) SC System Hysteresis

The original SCED brace was first developed by Christopoulos et al. [4] and extended by Erochko et al. [9]. To provide a restoring force, the SCED brace employs high strength tendons [9]. The detailed design, mechanics and behavior of SCED brace systems have been presented previously [9]. As shown in Fig. 2(a), a SCED brace consists of two rigid longitudinal members that are inner and outer steel members abutted by end plates at both ends, an energy dissipating device that is activated based on the relative movement between the inner and outer members, and pretensioned tendons which connect the two end plates and provide a restoring force once the gap between these longitudinal members opens.

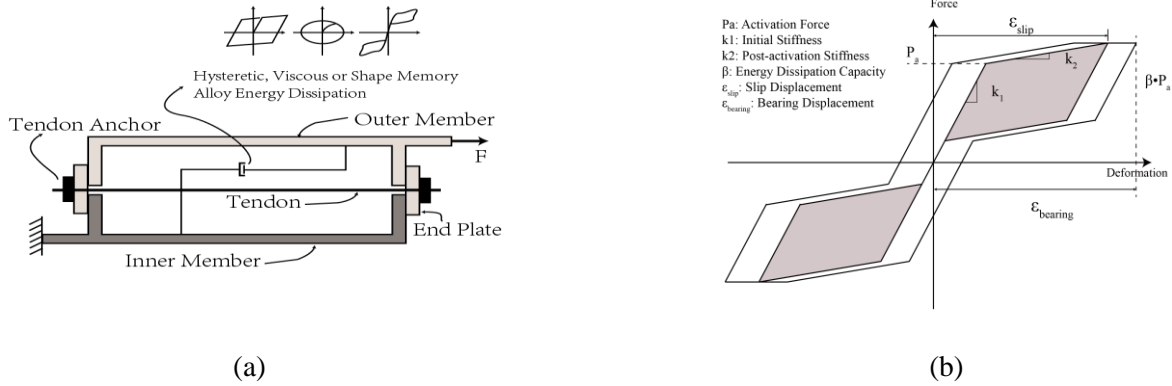


Fig. 2 - (a) Concept of SCED Brace (adapted from [9]); (b) Hysteretic Response of SCED Brace Model (adapted from [9])

The hysteretic response of the SCED model is shown in Fig. 2 (b). The behavior of the SCED brace is mainly controlled by the following parameters: (1) Activation force P_a ; (2) Initial stiffness k_1 ; (3) Post-activation stiffness k_2 ; (4) and the energy dissipation parameter β . These parameters will be varied in the design of the bridge to determine how they influence the performance of the retrofit.

3. Modeling of Bridge Structures

The first sample bridge is a two-span highway overpass with a continuous prestressed concrete deck and a supporting bent near center span composed of two circular columns with spiral reinforcement. The second sample bridge is a three-span highway overpass with similar bridge bent as the first bridge, located at approximate third spans. The deck of each bridge is supported on expansion bearings at abutments. The elevation, bent sections, dimensions and column cross section details are shown in Fig. 3(a) and (b).

Three-dimensional models of the sample bridges are analyzed using the structural analysis software OpenSEES [10]. Nonlinear push-over and time-history analyses of the sample bridges subjected to the two horizontal excitation components of a set of scaled earthquake records have been carried out. The records were scaled using the modal pushover scaling (MPS) method [11]. In MPS, the structure is idealized as a single degree of free (SDOF) system based on the modal pushover curve. Each pair of original excitations are multiplied a proper scaling factor such that the response of the SDOF is close to the target value.

The bridges are modeled using frame elements located at the centroids of structural members. Soil-structure interaction and second order effects are not considered. Rayleigh damping is adopted to provide 5% damping in the 1st and 12th modes. The bridge deck is assumed to remain elastic and is assumed to be fixed against vertical displacement and rotation about the longitudinal axis of the deck but free to move in both the longitudinal and transverse directions. The stiffness K_{abut} and capacity P_{bw} of abutment in the longitudinal direction are based on Caltrans Seismic Design Criteria [12]:

$$K_{abut} = K_i \times w \times \frac{h_{bw}}{1.7} \quad (\text{m, kN}) \quad (1)$$

$$P_{bw} = A_e \times 239 \text{ kPa} \times \frac{h_{bw}}{1.7} \quad (\text{m,kN}) \quad (2)$$

where K_i is the initial embankment fill stiffness, w is the width of the backwall, h_{bw} is the height of the backwall, and A_e is effective abutment wall area. According to SDC [12], K_i is taken as 14.35 kN/mm.

For a shear-wall type bridge abutment, the transverse stiffness of the abutment is much greater than that in the longitudinal direction even if the contribution from the wing walls is ignored. Thus in the model, the abutment is assumed to be fixed in the transverse direction. The shear key between the abutment and the bridge

deck can transmit the lateral forces generated by small to moderate earthquakes and service load; however, under stronger shaking of major earthquakes, the shear key may fail, after which the deck is free to move relatively to the abutment in the transverse direction. The shear key is modeled as an elastic-perfectly plastic element with small elastic deformation considering its low capacity.

The nonlinear behavior of the bridges is concentrated in the piers. In this analysis, the piers are assumed to be fixed in all degrees-of-freedom at the base and the pier columns are modeled using 3D fiber section nonlinear beam-column elements. As shown in Fig. 3(c), the piers are discretized into fibers including steel fibers, core concrete (confined concrete) fibers and cover concrete (unconfined concrete) fibers. The concrete material uses the Kent-Scott-Park concrete model [13]. The concrete tensile strength is ignored in this model. The confined concrete strength and strain capacity are determined using Mander’s Model [14]. The Chang and Mander [15] constitutive steel model is adopted to represent the behavior of steel.

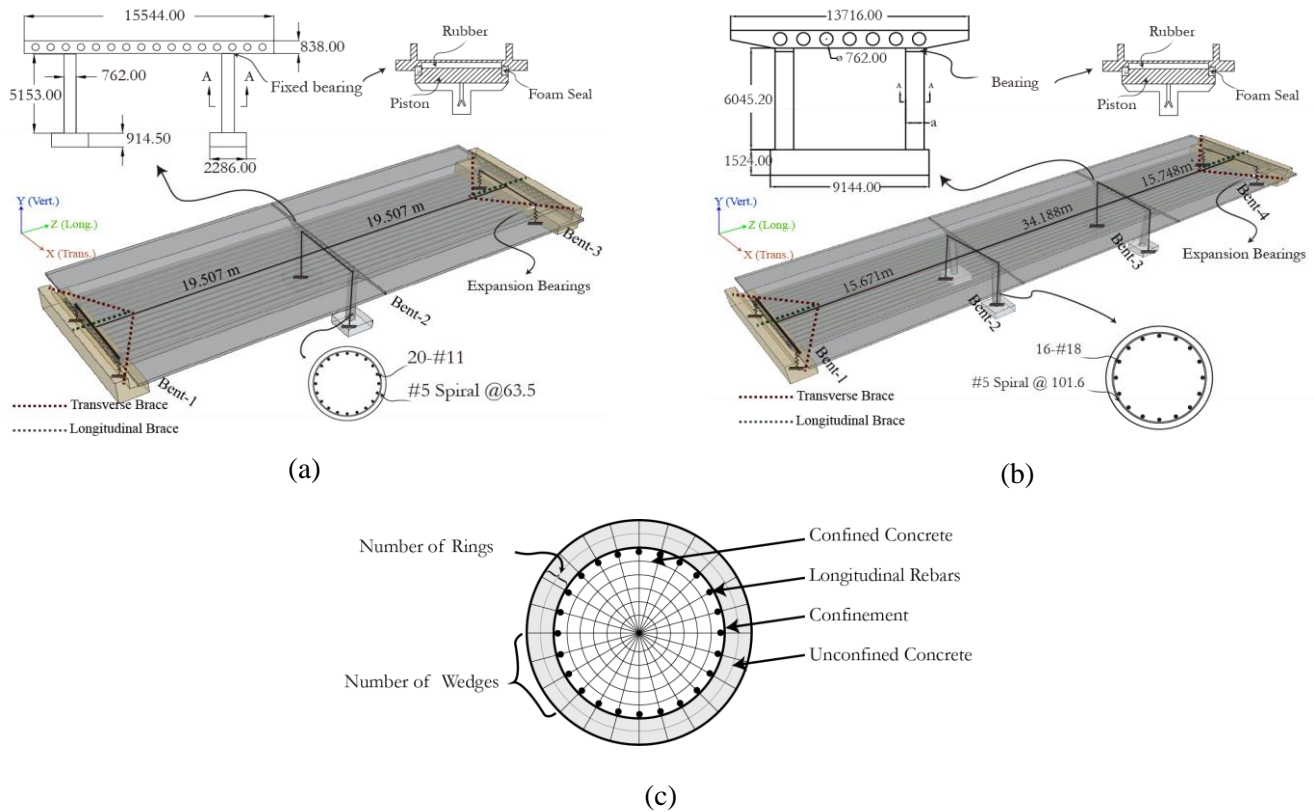


Fig. 3 – Details of Sample Overpass Bridges: (a) Two-Span Model; (b) Three-Span Model; (c) Fiber Section Model of Bridge Column

4. Modal Pushover Analysis (MPA) Results

The first two translational (longitudinal and transverse) modes of the two sample bridges are shown in Fig. 4. For the two-span bridge, the first two translational mode periods are 0.687 s and 0.442 s in the transverse and longitudinal direction, respectively. Correspondingly, the three-span bridge has 0.700 s and 0.325 s periods in the first and second mode, respectively.

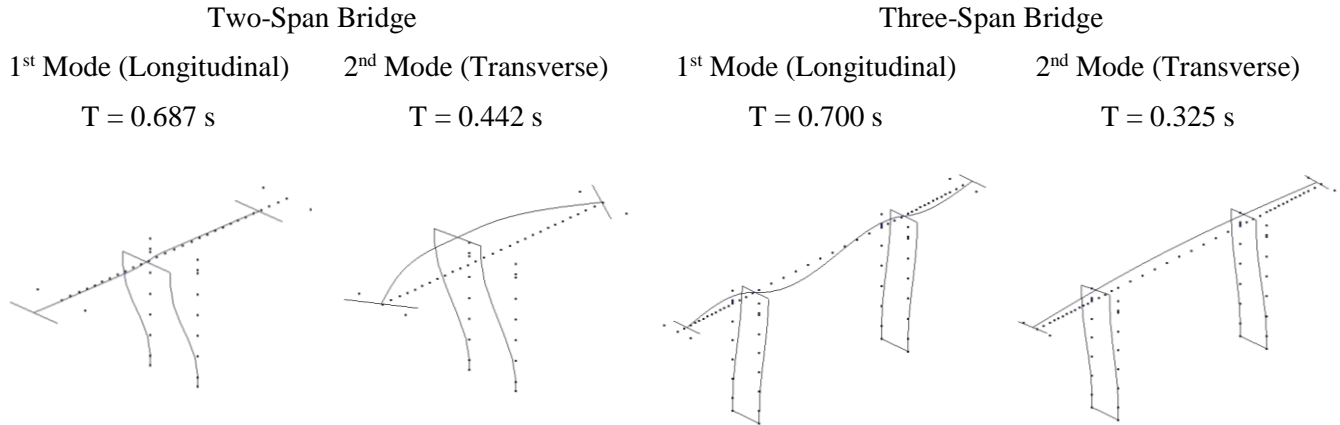


Fig. 4 – First Two Translational Modes of Vibration and Periods of The Sample Bridge Models

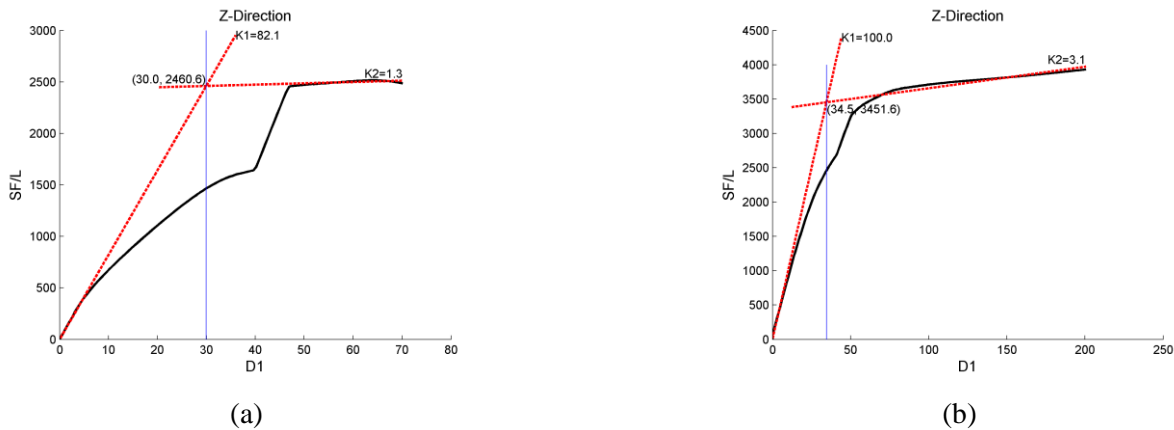


Fig. 5 – Modal Pushover Curves for Transverse and Longitudinal Direction of Sample Bridges: (a) Two-Span Model Pushover Curve; (b) Three-Span Model Pushover Curve;

In the modal pushover analysis, the invariant forces \mathbf{s}_n^* applied to the structure with respect to the n th mode is given by $\mathbf{s}_n^* = \mathbf{m}\phi_n$, where \mathbf{m} is structural mass matrix and ϕ_n is the n th mode shape. Modal pushover curves for the bridge are generated in the fundamental longitudinal direction; as a result, ϕ_n should be the fundamental longitudinal mode shape. The mid-span displacement at the bridge deck is taken as the earthquake displacement response demand. The idealized pushover curves for the fundamental longitudinal direction of the sample models are shown in Fig. 5 (a) and (b).

5. Ground Motions for Time-History Analysis (THA)

In performance-based design and evaluation methodologies, intensity-based scaling methods are preferred over spectral matching techniques which modify the original motion spectrum to match the target spectrum by modifying the frequency content or phasing of the record [11]. The modal pushover scaling (MPS) method [11] is adopted in this study.

Seven ground motion records from the set of ground motion records given in FEMA P695 [16] are used in this study as shown in Table 1. The FEMA P695 ground motion records are from 14 events that occurred between 1981 and 1999. Eight of these events took place in California and the rest were from different countries. Magnitudes of these events range from M6.5 to M7.6. The ground motion records are scaled (using MPS) to the seismic hazard level of 2% in 50 years for Victoria, BC in Canada according to NBCC 2015 [17]. They were scaled based on the first translational mode of the structure. Because the sample bridges are weaker in the longitudinal direction, the stronger horizontal component of each record is applied in the longitudinal direction to determine the most significant potential impact for retrofit using the self-centering braces. The resulting scaling factors are listed in Table 1. The response spectra for the selected records are shown in Fig. 6.

Table 1 – Scale Factors for Ground Motion Records

No.	Earthquake	Year	Station	Duration	Scaling Factor	
					1.00	2.00
1	Northridge	1994	Beverly Hills-Mulhol	30	0.88	1.00
2	Northridge	1994	Canyon Country-WLC	20	1.43	1.34
3	Kocaeli,Turkey	1999	Duzce	27	1.43	2.19
4	Landers	1992	Coolwater	28	1.05	1.53
5	Superstition Hills	1987	Poe Road	22	1.75	2.01
6	Cape Mendocino	1992	Rio Dell Overpass	36	1.94	2.38
7	San Fernando	1971	LA-Hollywood Stor	28	1.08	1.52

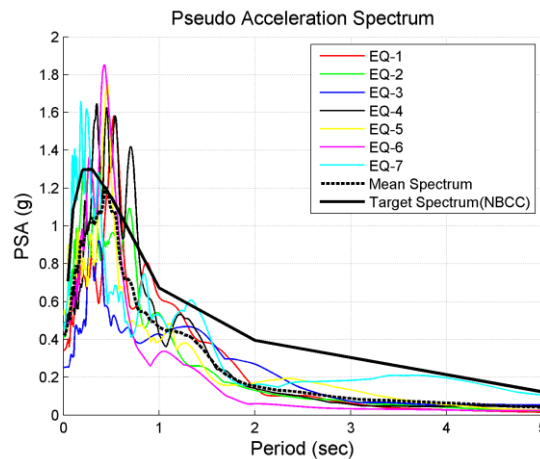


Fig. 6 - Unscaled Excitation Acceleration Spectrum for Components with Larger PGA

6. Analysis of Bridge Models

In this section, the behavior of the bridge with and without the self-centering braces are investigated. and how the properties of the SCED affect the performance of the retrofitted bridge are investigated.

In the current study, SCED braces are connected between the abutment or pier top to the bottom of the deck, as shown in Fig. 3 (a) and (b). The SCED braces can be categorized into two groups: transverse and longitudinal braces. The design of the SCED brace is an iterative process, and a full procedure for designing the SCED brace is described by Erochko [9]. In the design of these braces, the SCED brace target activation load P_a is initially equated to the demand load which is the maximum force the bridge abutment experiencing during the selected ground motions. The activation load P_a will be altered to make sure the braces can be activated during these ground motions. The energy dissipation capacity β typically varies between 0.85 and 0.95.

As determined from the modal analysis, both sample bridges are relatively less stiff in the longitudinal direction. Under bidirectional excitations, the relative longitudinal displacement between the abutment and the deck is thus expected to be greater than that in the transverse direction. Since the larger relative displacement in the longitudinal direction of the SCED braces can generate greater restoring forces and higher damping, the reduction in peak longitudinal displacement and residual longitudinal displacement of the retrofitted bridge should be more pronounced than that in the transverse direction, where there is limited lateral movement in the abutment until the shear keys fail.

The brace properties determined for the sample bridge models are presented in Table 2. As indicated in Fig. 2 (b), the behavior of the SCED brace is mainly controlled by activation force P_a , initial stiffness k_1 , post-activation stiffness k_2 (or k_2/k_1) and energy dissipation capacity β . In this study, the optional external fuse is not considered and as a result, the bearing deformation $\epsilon_{bearing}$ is not investigated. The activation force P_a , initial stiffness k_1 , post-activation stiffness k_2 (or k_2/k_1) and energy dissipation capacity β for cases 1 to 9 of different SCED brace design are shown in Table 2. The initial stiffness assigned to the SCED braces makes sure that the braces can be activated before the deck pounds the abutment. For each design case, all of the selected scaled ground motion records were used as input excitations in the analysis of the bridges.

Table 2 – SCED Brace Properties in the Sample Bridge Models

Model	Two-Span Model									Three-Span Model								
Case	1	2	3	4	5	6	7	8	9	1	2	3	4	5	6	7	8	9
Position	Transverse [Longitudinal]									Transverse [Longitudinal]								
Length (mm)	5368 [4572]									5859 [5000]								
P_a (kN)	1000	1100	1200	1000		1000		1000		3000	3100	3200	3000		3000		3000	
k_1	100			120	150	100		100		200			210	220	200		200	
k_2/k_1	0.075			0.075		0.08	0.09	0.075		0.075			0.075		0.08	0.085	0.075	
β	0.9			0.9		0.9		0.92	0.95	0.9			0.9		0.9		0.92	0.95

7. Peak Displacements

The peak displacement of the sample bridge models are compared in Fig. 7 for all the maximum credible earthquake (MCE) records. Generally, peak displacement can be reduced with the help of the retrofit both in longitudinal and transverse direction. For instance, as shown in Fig. 7 (b), the average peak displacement of the unretrofitted two-span model is 102 mm. After the retrofit, it is reduced to 54 mm, which is approximate half of that without retrofit. In three-span model, the peak longitudinal displacement is reduced by 40%. The maximum peak transverse displacements of two-span model occur at Bent 2 and is found to reduce to 90% with the retrofit. The small reduction at mid spans in transverse direction reveals that some SCED braces should be assigned to them. As expected, the reduction in peak transverse displacement is not as effective as that in the longitudinal direction due to smaller damping and restoring forces provided by SCED braces in the transverse direction.

However, it is recognized that the peak displacement of the retrofit structure can sometimes be greater than that of the unretrofitted structure. The external SCED brace elements added to the structure can shift the fundamental periods of the structure resulting in larger peak displacement responses. As can be seen from Fig. 6, the response spectrum of MPS-6 has a peak at 0.4 s, which is close to the fundamental period (in the longitudinal direction) of the retrofitted structure. As a result, the peak longitudinal displacements under MPS-6 is greater than that of the unretrofitted structure.

The mean and displacement of the peak displacements under each EQ from Case 1 to Case 9 are also plotted in Fig. 7 and compared in Table 3. The dark blue and dark red bars on the left edge in each subplot represent mean peak displacements and standard deviation, respectively. By comparing the performance of every

design case of the SCED brace systems, it is concluded that by increasing k_1 , k_2 and β can reduce the peak displacements. There is no strong correlation between P_a and peak displacement.

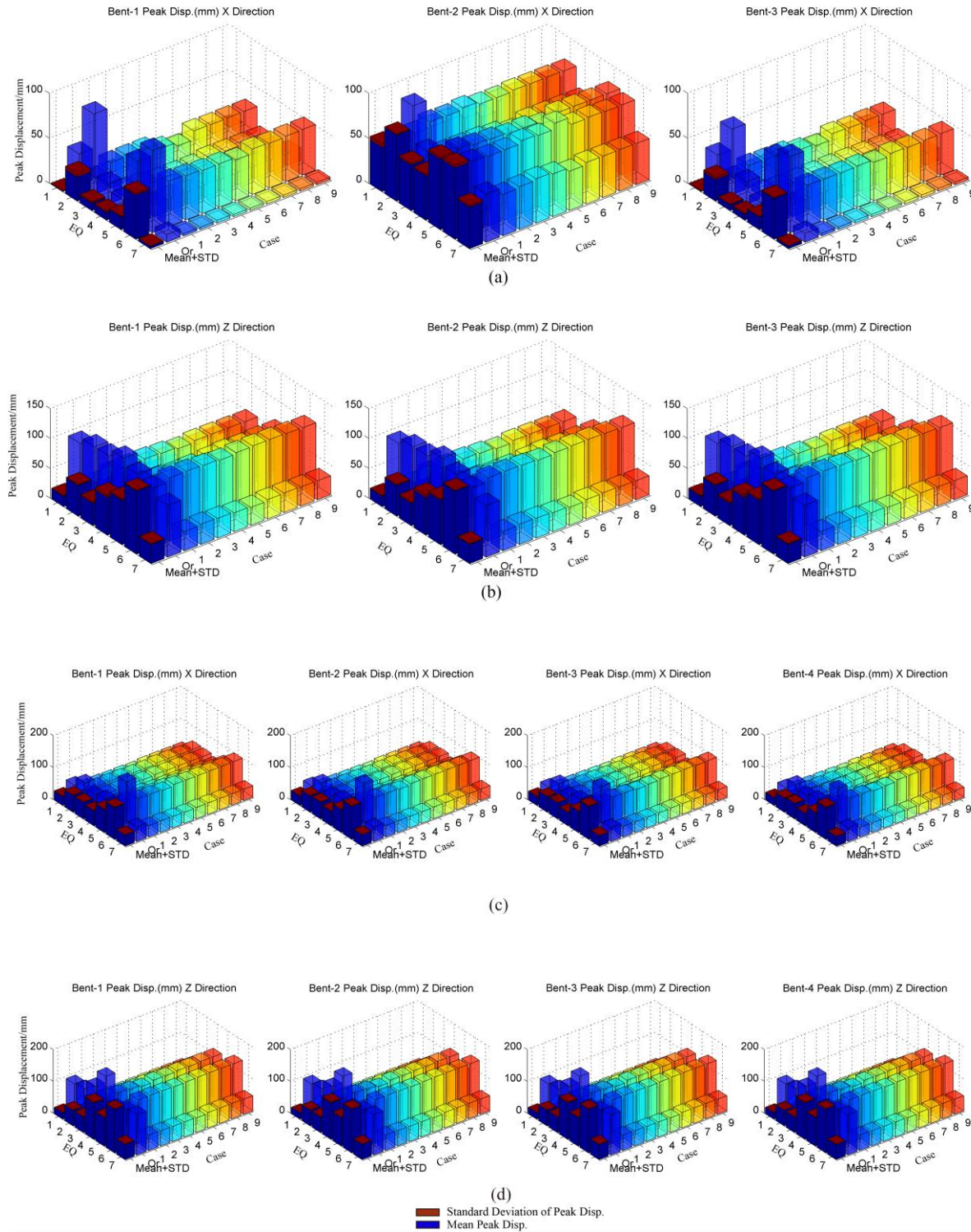


Fig. 7 – Peak Displacement Comparison: (a) Transverse and (b) Longitudinal for Two-Span Model; (c) Transverse and (d) Longitudinal for Three-Span Model

Table 3 – Mean and Standard Deviation of Peak Displacement

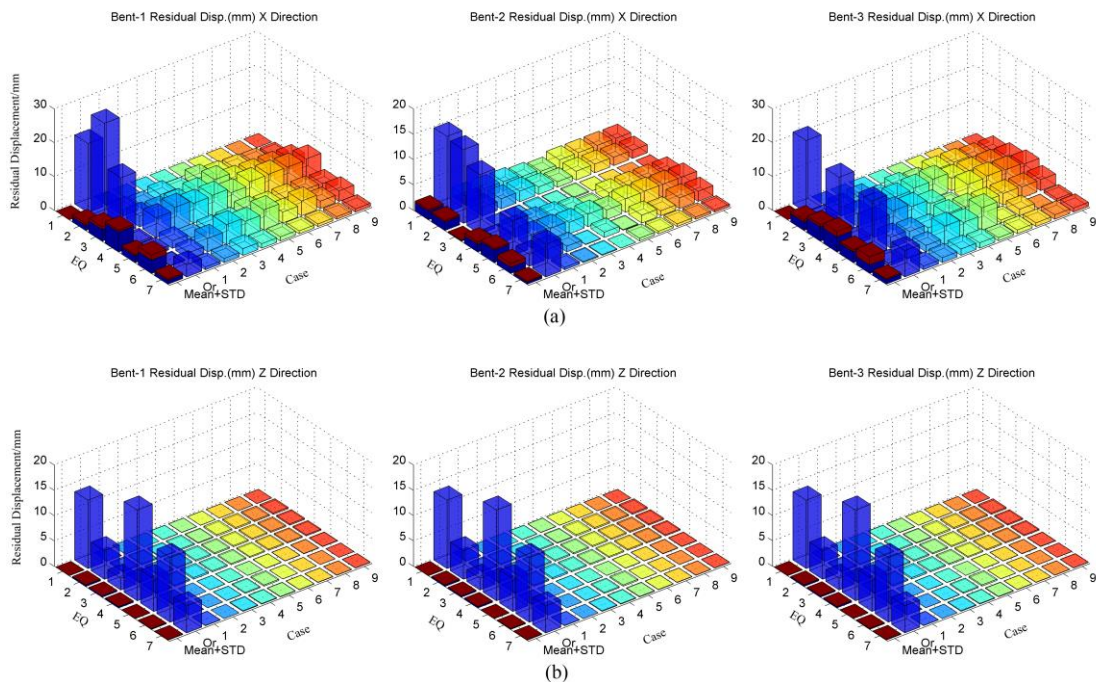
EQ	Two Span Model								Three Span Model									
	X						Z		X								Z	
	Bent-1		Bent-2		Bent-3		Bent-1 to 3		Bent-1		Bent-2		Bent-3		Bent-4		Bent-1 to 4	
	M.	Std.	M.	Std.	M.	Std.	M.	Std.	M.	Std.	M.	Std.	M.	Std.	M.	Std.	M.	Std.
1	1	0	49	4	1	0	17	1	28	1	29	1	27	1	23	1	20	0
2	27	4	73	1	24	2	51	1	52	1	51	1	48	0	44	1	49	0
3	8	1	51	2	7	0	37	2	52	1	53	0	51	0	48	1	49	0
4	9	1	49	2	7	1	63	4	47	1	46	1	42	0	39	0	114	2
5	14	0	79	2	14	0	74	2	72	1	72	1	67	0	62	1	90	1
6	49	2	79	3	45	1	105	1	99	1	102	1	102	2	99	2	137	1
7	3	0	46	2	3	0	32	1	35	0	36	0	33	0	30	0	47	1

Note: M.= Mean Value; Std.=Standard Deviation; All the values are in mm.

8. Residual Displacements

It is recognized that both peak displacement and residual displacement are important parameters for consideration in seismic design. For lifeline structures, such as post-disaster bridges, it is critically important that the residual displacements after an earthquake be small such that they do not impair immediate traffic operation of the bridge. The set defined relationship between the level of residual displacement and its consequence to the operation and functional capacities of a structure is not yet defined, but the relationship in buildings has been discussed qualitatively in [18] and [19]. For the case of buildings of residual drift less than 0.5%, it is not necessary to conduct an intervention in most cases. For residual drift between 0.5% and 1.0%, an assessment is required before reoccupation. For residual drift between 1.0% and 1.5%, the structure needs to be straightened or reinforced at the deformed position. If residual drift is greater than 1.5%, the structure loses its functionality from an economic perspective.

Similarly in previous section, the mean and standard deviation of the residual displacements are also compared in Fig. 8 and Table 4.



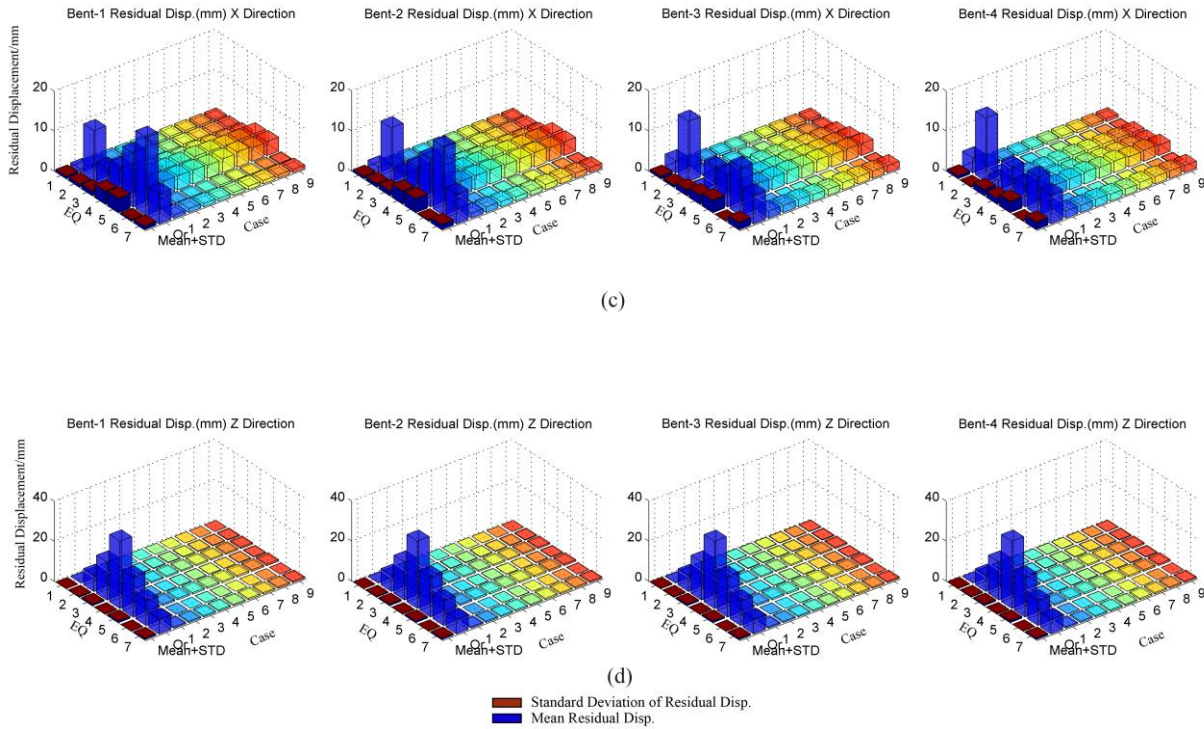


Fig. 8 – Residual Displacement Comparison: (a) Transverse and (b) Longitudinal for Two-Span Model; (c) Transverse and (d) Longitudinal for Three-Span Model

Table 4 - Mean and Standard Deviation of Residual Displacement

	Two Span Model								Three Span Model									
	X				Z				X								Z	
	Bent-1		Bent-2		Bent-3		Bent-1 to 3		Bent-1		Bent-2		Bent-3		Bent-4		Bent-1 to 4	
EQ	M.	Std.	M.	Std.	M.	Std.	M.	Std.	M.	Std.	M.	Std.	M.	Std.	M.	Std.	M.	Std.
1	0	0	2	0	0	0	0	0	1	0	1	0	1	0	1	0	0	0
2	1	1	2	0	2	1	0	0	1	0	1	0	0	0	0	0	0	0
3	3	1	0	0	4	1	0	0	1	0	1	0	1	0	1	0	1	0
4	6	1	2	1	4	2	0	0	3	0	3	0	2	0	1	0	0	0
5	2	1	3	0	3	1	0	0	3	0	3	0	3	0	3	0	1	0
6	4	1	1	1	2	2	0	0	0	0	0	0	0	0	0	0	0	0
7	1	0	0	0	1	0	0	0	1	0	1	0	2	0	2	0	1	0

Note: M.= Mean Value; Std.=Standard Deviation; All the values are in mm.

For the study here, the residual displacement of the sample bridges subjected to the MCE are compared in Fig. 8. For both sample bridge models, it is evident that longitudinal residual displacements of the retrofitted bridges are reduced to negligible level. However, residual displacement is not only dependent on the structure properties. The symmetry of the input ground motion will affect it as well. For instance, both of the unretrofitted bridges have larger transverse residual displacement when they are subjected to MPS-4. It can be observed from the MPS-4 acceleration time history plots shown in Fig. 9, that the transverse input ground motion has a higher accelerations in the positive direction. This phenomenon can also be observed in MPS-6. Whereas, the

longitudinal input ground motion of MPS-4 shows more symmetric shape. As a result, unretrofitted structures subjected to MPS-4 have larger transverse residual displacement. As previously mentioned, SCED braces have less effect in the transverse direction. Thus, the transverse residual displacement is greater than longitudinal residual displacements. Even so, after retrofitting using SCED braces, the transverse residual displacements are reduced enough that they can be easily accommodated by the bridges. As shown in Fig. 8, by increasing k_1 , k_2 and β , residual displacements can be reduced.

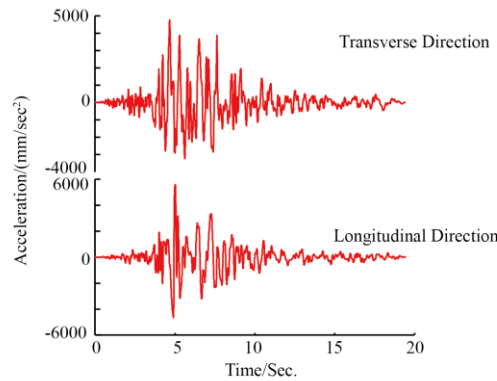


Fig. 9 – MPS-4 Acceleration Time History

9. Conclusions

This study show the effect of retrofitting 3D bridge models using SCED braces with different properties. The braces were only located at the abutments in longitudinal and transverse direction. To conduct time history analysis, all the selected ground motion records were scaled to MCE level using MPS method. The original and retrofitted bridge models were subjected to these scaled ground motions. The performance of the retrofitted bridges with self-centering brace systems was found to be much improved with lower maximum superstructure displacements low residual displacements. The effects of different SCED brace systems by varying the SCED design parameters (activation force P_a , initial stiffness k_1 , post-activation stiffness k_2 (or k_2/k_1) and energy dissipation capacity β) are investigated.

It was shown that increasing k_1 , k_2 and β can reduce both the peak displacement and residual displacement. But there is no definite correlation shown between peak or residual displacement and the activation force P_a ; however, a future study should consider a wider range of activation force values.

Because the ground motions are scaled based on the first mode, which is in the longitudinal direction, the longitudinal response under every ground motion record is around the same level. The larger response in the longitudinal direction tends to induce greater damping and force in this direction if all the braces have same properties in each trial. As a result, these SCED braces can provide better protection in the longitudinal direction. To improve the retrofit performance in the transverse direction, the transverse SCED braces should have higher strength in terms of stiffness and damping. It was also found that the retrofit alters the fundamental period of the structure and resonance may take place and increase the peak displacement.

The results presented in this paper demonstrate the benefits of retrofitting bridges using SCED braces. These SCED braces can strengthen the structure and dissipate energy. This reduces the peak displacements and makes sure the residual displacements are limited to increase the likelihood that the bridge will be usable after a seismic event.

Reference

- [1] Priestley MJN, Seible F, Calvi GM (1996): *Seismic Design and Retrofit of Bridges*, John Wiley & Sons.



- [2] Erochko J, Christopoulos C, Tremblay R (2014): Design and testing of an enhanced-elongation telescoping self-centering energy-dissipative brace, *Journal of Structural Engineering*, **141**(6), 04014163.
- [3] Vishnukanthan K (2013): Probabilistic performance-based seismic risk assessment of bridge inventories with loss and impact estimates, Carleton University, CA.
- [4] Christopoulos C, Tremblay R, Kim H-J, Lacerte M (2008): Self-centering energy dissipative bracing system for the seismic resistance of structures: development and validation, *Journal of Structural Engineering*, **134**(1), 96–107.
- [5] Hewes JT, Priestley MJN (2002): Seismic design and performance of precast concrete segmental bridge columns. *UCSD /SSRP-2001/25*.
- [6] Kwan W, Billington SL (2003): Unbonded posttensioned concrete bridge piers I: monotonic and cyclic analyses, *Journal of Bridge Engineering*, **8**(April), 92–101.
- [7] Mander JB, Cheng CT (1997): Seismic resistance of bridge piers based on damage avoidance design. *Technical Report NCEER 1997*.
- [8] Christopoulos C, Filiatrault A (2006): *Principles of Passive Supplemental Damping and Seismic Isolation*, IUSS Press.
- [9] Erochko JA. (2013): Improvements to the design and use of post-tensioned self-centering energy-dissipative (SCED) braces, University of Toronto, CA.
- [10] Mazzoni S, McKenna F, Scott MH, Fenves GL (2006): OpenSees command language manual, *Pacific Earthquake Engineering Research (PEER) Center*, US National Center for Earthquake Engineering Research (NCEER), USA.
- [11] Kalkan E, Chopra AK (2010): Practical guidelines to select and scale earthquake records for nonlinear response history analysis of structures. *US Geological Survey Open-File Report 2010*, USA.
- [12] Caltrans (2013): Seismic Design Criteria Version 1.7, *California Department of Transportation: Sacramento, CA, U.S.*
- [13] Kent DC, Park R (1971): Flexural Members with Confined Concrete, *Journal of the Structural Division*, **97**(7), 1969–1990.
- [14] Mander JB, Priestley MJ, Park R (1988): Theoretical Stress-strain Model for Confined Concrete, *Journal of Structural Engineering*, **114**(8), 1804–1826.
- [15] Chang G a, Mander JB (1994): Seismic energy based fatigue damage analysis of bridge columns : part 1 - evaluation of seismic capacity, *Technical Report NCEER*, State University of New York, Buffalo, New York, USA.
- [16] Federal Emergency Management Agency (FEMA) (2009): Quantification of building seismic performance factors.
- [17] National Research Council of Canada [NRC] (2015): National Building Code of Canada, National Research Council of Canada, Ottawa, Canada.
- [18] Choi H, Erochko J, Christopoulos C, Tremblay R (2008): Comparison of the seismic response of steel buildings incorporating self-centering energy dissipative braces , buckling restrained braced and moment resisting frames, *The 14-Th World Conference on Earthquake Engineering*, Beijing, China.
- [19] Erochko J, Christopoulos C, Tremblay R, Choi H (2010): Residual drift response of SMRFs and BRB frames in steel buildings designed according to ASCE 7-05, *Journal of Structural Engineering*, **137**(5), 589–599.